

# Impaired KIN10 function restores developmental defects in the *Arabidopsis trehalose 6-phosphate synthase1 (tps1)* mutant

Vasiliki Zacharaki<sup>1\*</sup> , Jathish Ponnu<sup>2,3\*</sup> , Nathalie Crepin<sup>4,5</sup> , Tobias Langenecker<sup>2</sup> , Jörg Hagmann<sup>2</sup> ,  
Noemi Skorzinski<sup>1,2</sup> , Magdalena Musialak-Lange<sup>6</sup> , Vanessa Wahl<sup>6</sup> , Filip Rolland<sup>4,5</sup>  and  
Markus Schmid<sup>1,2</sup> 

<sup>1</sup>Department of Plant Physiology, Umeå Plant Science Centre, Umeå University, SE-901 87 Umeå, Sweden; <sup>2</sup>Department of Molecular Biology, Max Planck Institute for Developmental Biology, Spemannstr. 35, 72076 Tübingen, Germany; <sup>3</sup>Institute for Plant Sciences, Cologne Biocenter, Universität zu Köln, Zùlpicher StraÙe 47b, 50674 Köln, Germany; <sup>4</sup>Laboratory for Molecular Plant Biology, Biology Department, University of Leuven–KU Leuven, Kasteelpark Arenberg 31, 3001 Heverlee-Leuven, Belgium; <sup>5</sup>KU Leuven Plant Institute (LPI), 3001 Heverlee-Leuven, Belgium; <sup>6</sup>Department of Plant Reproductive Biology and Epigenetics, Max Planck Institute of Molecular Plant Physiology, Am Mùhlenberg 1, 14476 Potsdam, Germany

## Summary

Authors for correspondence:

Markus Schmid

Email: markus.schmid@umu.se

Filip Rolland

Email: filip.rolland@kuleuven.be

Received: 28 September 2021

Accepted: 9 March 2022

*New Phytologist* (2022) **235**: 220–233

doi: 10.1111/nph.18104

**Key words:** *Arabidopsis thaliana*, embryogenesis, flowering time, SnRK1 complex, TPS1, T6P pathway.

- Sensing carbohydrate availability is essential for plants to coordinate their growth and development. In *Arabidopsis thaliana*, TREHALOSE 6-PHOSPHATE SYNTHASE 1 (TPS1) and its product, trehalose 6-phosphate (T6P), are important for the metabolic control of development. *tps1* mutants are embryo-lethal and unable to flower when embryogenesis is rescued. T6P regulates development in part through inhibition of SUCROSE NON-FERMENTING1 RELATED KINASE1 (SnRK1).
- Here, we explored the role of SnRK1 in T6P-mediated plant growth and development using a combination of a mutant suppressor screen and genetic, cellular and transcriptomic approaches.
- We report nonsynonymous amino acid substitutions in the catalytic KIN10 and regulatory SNF4 subunits of SnRK1 that can restore both embryogenesis and flowering of *tps1* mutant plants. The identified SNF4 point mutations disrupt the interaction with the catalytic subunit KIN10.
- Contrary to the common view that the two *A. thaliana* SnRK1 catalytic subunits act redundantly, we found that loss-of-function mutations in KIN11 are unable to restore embryogenesis and flowering, highlighting the important role of KIN10 in T6P signalling.

## Introduction

Flowering is an important process in the life cycle of plants and involves major physiological changes (Srikanth & Schmid, 2011; Romera-Branchat *et al.*, 2014; Song *et al.*, 2015). Flowering time in *Arabidopsis thaliana* is under the control of several stimuli which are integrated in a complex genetic network that converges on floral integrator genes such as the florigen *FLOWERING LOCUS T (FT)* and *SUPPRESSOR OF OVEREXPRESSION OF CO 1 (SOC1)*, which in turn control the expression of floral meristem identity genes such as *LEAFY (LFY)* and *APETALA1 (API)*. Once activated, flowering commences with the induction of floral meristems at the flank of the shoot meristem, followed by internode elongation, or bolting.

Daylength is among the most important factors affecting flowering time. In *A. thaliana*, flowering is accelerated in response to long days (LD) and is under the regulation of the circadian clock,

which regulates *CONSTANS (CO)* expression during the day with CO in turn activating *FT* transcription (Srikanth & Schmid, 2011; Romera-Branchat *et al.*, 2014; Song *et al.*, 2015). Plant age governs flowering mainly by the function of two microRNAs, miR156 and miR172 (Huijser & Schmid, 2011). As plants mature, miR156 levels decrease, resulting in an upregulation of *SQUAMOSA PROMOTER BINDING-LIKE (SPL)* genes. SPL transcription factors promote flowering directly by activating the floral homeotic genes, and indirectly by inducing miR172, which represses *APETALA2-like (AP2)* floral repressors.

Carbohydrate availability has also been implicated in the transition from vegetative to reproductive development. Of particular importance in this regard is the phospho-disaccharide trehalose 6-phosphate (T6P) (Cabib & Leloir, 1958). T6P plays a key role in signalling carbohydrate availability in plants, thereby regulating a large number of physiological and developmental responses (Eastmond *et al.*, 2002; Schluepmann *et al.*, 2003; van Dijken *et al.*, 2004; Gomez *et al.*, 2006, 2010; Lunn *et al.*, 2006; Satoh-Nagasawa *et al.*, 2006; Wingler *et al.*, 2012; Wahl *et al.*, 2013;

\*These authors contributed equally to this work.

Ponnu *et al.*, 2020). Furthermore, T6P has been implicated in the feedback regulation of sucrose concentrations by restricting sucrose synthesis and/or promoting sucrose consumption, forming a robust T6P–sucrose nexus (Lunn *et al.*, 2014; Yadav *et al.*, 2014).

In plants, T6P synthesis is catalysed by TREHALOSE PHOSPHATE SYNTHASE (TPS) proteins. In *A. thaliana*, TPS1 is the major active isoform (Vandesteene *et al.*, 2010; Yang *et al.*, 2012; Fichtner *et al.*, 2020). Consistently, homozygous *A. thaliana tps1* mutants (*tps1-2*) display embryo-lethality (Eastmond *et al.*, 2002). However, when embryo lethality is bypassed by ectopically expressing dexamethasone (DEX)-inducible *TPS1* (*GVG::TPS1*) during seed set (van Dijken *et al.*, 2004; Wahl *et al.*, 2013), homozygous *tps1-2* plants that remain in the vegetative phase and fail to flower can be recovered. Thus, TPS1 catalytic activity is critical for the metabolic control of key plant developmental processes and transitions (Fichtner *et al.*, 2020).

T6P regulates development in part through SnRK1. SnRK1 is a heterotrimeric kinase complex that acts as a sugar/energy sensor and is required for normal plant function and for plant responses to various stress conditions that affect energy homeostasis and thereby plant fitness and survival (Polge & Thomas, 2007; Baena-Gonzalez & Sheen, 2008). SnRK1 is a structural and functional homologue of the low-energy stress-activated yeast SNF1 and animal AMP-activated kinase (AMPK). The AMPK/SNF1/SnRK1 kinase complexes are typically composed of three different subunits: a catalytic  $\alpha$  subunit (SnRK1 $\alpha$ 1/KIN10 or SnRK1 $\alpha$ 2/KIN11 in *A. thaliana*), a regulatory  $\beta$  subunit and a regulatory  $\gamma$  subunit (Hedbacker & Carlson, 2008; Ghillebert *et al.*, 2011; Hardie *et al.*, 2012; Broeckx *et al.*, 2016). The catalytic subunits contain a highly conserved N-terminal serine/threonine kinase domain, with an activation or T-loop that requires phosphorylation for kinase activity, and a large C-terminal regulatory domain for interaction with the other subunits (Estruch *et al.*, 1992; Hawley *et al.*, 1996; Baena-Gonzalez *et al.*, 2007). The T-loop (Thr175 in KIN10) is phosphorylated by the upstream SnRK1 activating kinases, SnAK1/GRIK2 and SnAK2/GRIK1 (Kong & Hanley-Bowdoin, 2002; Shen & Hanley-Bowdoin, 2006; Shen *et al.*, 2009; Crozet *et al.*, 2010; Glab *et al.*, 2017), but also shows significant autophosphorylation (Baena-Gonzalez *et al.*, 2007; Ramon *et al.*, 2019). In *A. thaliana*, KIN10 is broadly expressed and believed to be responsible for most of the SnRK1 kinase activity (Jossier *et al.*, 2009; Williams *et al.*, 2014). The  $\beta$ -subunits (KIN $\beta$ s) act as complex scaffolds but also control kinase activity, substrate specificity and localization (Hedbacker *et al.*, 2004; Polge & Thomas, 2007; Ghillebert *et al.*, 2011; Emanuelle *et al.*, 2015; Ramon *et al.*, 2019). In plants, a single hybrid  $\beta\gamma$  subunit (SNF4 in *A. thaliana*) acts as the complex  $\gamma$  subunit (Ramon *et al.*, 2013). *SNF4* is an essential gene as no homozygous loss-of-function mutants were obtained (Ramon *et al.*, 2013; Gao *et al.*, 2016). The  $\beta\gamma$  subunit consists of a conserved  $\gamma$  subunit domain with four cystathionine  $\beta$ -synthase (CBS) motifs and a carbohydrate-binding module (CBM), typically only found in the  $\beta$  subunits in nonplant species.

In AMPK and SNF1, the  $\gamma$  subunit acts as the energy-sensing module, competitively binding AMP, ADP and ATP. However, in plants nucleotide charge does not have an important regulatory signal (Ramon *et al.*, 2013; Emanuelle *et al.*, 2015). Instead,

SnRK1 is active by default and inhibited by high energy availability (Ramon *et al.*, 2019). Sugars such as sucrose and glucose suppress SnRK1 activity (Baena-Gonzalez *et al.*, 2007) and this repressive effect can be attributed at least in part to T6P, which (as a proxy for high sugar availability) was identified as an allosteric inhibitor of SnRK1 (Zhang *et al.*, 2009). More recently, T6P was suggested to directly bind to KIN10 and interfere with its binding and phosphorylation by the upstream kinases (Zhai *et al.*, 2018). In response to activation (derepression) by low energy status (e.g. in extended darkness), SnRK1 phosphorylates a range of enzymes and transcription factors to reprogram metabolism and gene expression. Direct activation of C- and S1-class bZIP transcription factor dimers, for example, induces the expression of genes such as *DARK INDUCED6/ASPARAGINE SYNTHASE1* (*DIN6/ASN1*) and *SENESCENCE5* (*SEN5*), which can be used to monitor SnRK1 activity (Baena-Gonzalez *et al.*, 2007; Delatte *et al.*, 2011; Dietrich *et al.*, 2011; Mair *et al.*, 2015).

The role of the T6P pathway in flowering time control has been mainly associated with *FT* induction in leaves and the age pathway and miR156 expression in the shoot apical meristem (SAM) (Wahl *et al.*, 2013). To identify mutations that rescue the nonflowering phenotype, *tps1-2 GVG::TPS1* seeds were mutagenized with ethyl methanesulfonate (EMS).

We expected to recover (at least) two categories of mutants from this screen: bypass mutations, which would restore flowering to *tps1-2* but were not necessarily involved in T6P signalling, and mutations that would interfere with T6P signalling downstream of TPS1. Here we describe the identification of several alleles with amino acid substitutions in the SnRK1 subunits KIN10 and SNF4 that can restore both flowering and embryogenesis in *tps1-2* plants. We found that flowering rescue requires both an early induction of *FT* in the leaves and a later decrease of miR156 and subsequent induction of *SPLs* in the SAM. All newly identified *kin10* alleles have mutations in the catalytic domain C-lobe. While the mutated G163 and G178 residues are located in or near the catalytic cleft (with the conserved T176 in the activation- or T-loop), mutation of the R259 residue, which is more distant from the T-loop in the primary protein sequence but in close spatial proximity (Broeckx *et al.*, 2016; Jumper *et al.*, 2021), might affect activity more indirectly. The single amino acid substitutions in SNF4 abolish or reduce interaction with KIN10, thereby also affecting SnRK1 complex function. Importantly, mutations in KIN11 were unable to rescue the *tps1-2* mutant. Our results demonstrate that loss of KIN10, but not KIN11, can restore flowering and embryogenesis in the *tps1-2* mutant, providing a clear genetic link between the T6P pathway and KIN10, and indicate that KIN10–SNF4 interaction is required for adequate SnRK1 activity in *planta*.

## Materials and Methods

### Plant materials and growth conditions

All plants are *A. thaliana* in the Col-0 background. The *tps1-2*, *tps1-2 GVG::TPS1*, *ft-10* (*GABI\_290E08*) and *snrk1 $\alpha$ 1-3* (*GABI\_579E09*) mutants have been described (Eastmond *et al.*, 2002; van Dijken *et al.*, 2004; Yoo *et al.*, 2007; Mair *et al.*, 2015).

*kin11cr* mutants were created by CRISPR/Cas9 using the pHSE401 binary vector (Xing *et al.*, 2014) and gRNA1 and gRNA2 (Supporting Information Table S1; Fig. S1). Plants were grown on soil under wide photosynthetically active radiation (PAR) spectrum LED lights (110–130  $\mu\text{mol m}^{-2} \text{s}^{-1}$ ; CLF Plant Climatics, Wertingen, Germany) under LD (16 h : 8 h, light : dark) or short day (SD, 8 h : 16 h, light : dark) conditions, 65% relative humidity and 23°C. For dark-induced starvation, plants grown for 14 d in LD were exposed to an additional 12 h of darkness before harvesting under green light. Plants for the RNA-sequencing (RNA-seq) experiment were grown in different cabinets from the flowering time experiments, but with CLF wide PAR spectrum LED lights (110–130  $\mu\text{mol m}^{-2} \text{s}^{-1}$ ) and the same conditions and settings. All newly characterized *kin10* and *snf4* mutations were confirmed by genotyping. See Methods S1 for details.

### EMS mutagenesis of *tps1-2 GVG:TPS1* and identification of suppressor mutants

Around 15 000 *tps1-2 GVG:TPS1* seeds were stratified at 4°C for 3 d before being treated with 25 ml of 0.4% EMS (Sigma) as described (Weigel & Glazebrook, 2002). M1 plants were grown on soil and sprayed with 1  $\mu\text{M}$  DEX (Sigma) solution containing 0.02% Tween-20 (Sigma) at 2 d intervals from 10 d after sowing (DAS). M2 seeds were collected as 300 pools of 40–50 M1 plants. Approximately 500 M2 plants were grown from each M2 pool under LD at 23°C and screened for mutants that flowered without application of DEX. The phenotype and the homozygous state of the *tps1-2* transposon insertion were confirmed in the M3 generation by genotyping using primers 366, 367 and 368 (Table S1).

### Mapping by sequencing

Mapping of EMS-induced single nucleotide polymorphisms (SNPs) and statistical analyses were performed as previously described (Ossowski *et al.*, 2008; Schneeberger *et al.*, 2009). For details see Methods S2.

### Flowering and bolting time measurement

Flowering and bolting time were measured by counting the number of days when inflorescences reach 1 cm (bolting) after sowing and the total number of leaves originating from the main shoot meristem, respectively. A minimum of 15 plants from different seed batches were used for each genotype per experiment. Error bars represent the standard deviation (SD) of mean values and letters the statistical differences among the genotypes based on ANOVA and Tukey's HSD test.

### RT-qPCR and RNA-seq data analyses

RNA for real-time quantitative PCR (RT-qPCR) was extracted using a RNeasy Plant Mini Kit (Qiagen) or TRIzol<sup>®</sup> Reagent (Invitrogen). cDNA was synthesised using the RevertAid First

Strand cDNA Synthesis Kit (Thermo Scientific, Waltham, MA, USA) and qPCR was performed on a Bio-Rad CFX96 instrument. Primers used for RT-qPCR are listed in Table S1. For a detailed description of the RT-qPCR analysis and RNA-seq data preprocessing, differential expression and differential usage analyses see Methods S3, S4.

### RNA *in situ* hybridization

RNA *in situ* hybridization using a specific *SOC1* antisense probe was carried out as previously described (Wahl *et al.*, 2013; Olas *et al.*, 2019). For details see Methods S5.

### Vectors and cloning

For yeast-two-hybrid (Y2H) assays, the original pGADT7 and pGBKT7 vectors from Clontech/Invitrogen were modified to make them compatible with GreenGate (GG) cloning system 'C' modules (Lampropoulos *et al.*, 2013). *EcoR31I* (or *BsaI*) sites were introduced into pGADT7 and pGBKT7 after the AD or BD, respectively, and a *ccdB* cassette and a chloramphenicol resistance gene were added between the *EcoR31I* sites. *EcoR31I* sites present in the backbone of pGADT7 and pGBKT7 were mutagenized by site-directed mutagenesis. The final newly designed GreenGate-compatible BD and AD vectors designated as pVZ022-AD and pVZ023-BD were verified by sequencing. PCR-amplified and gel-purified products were introduced into pVZ022-AD and pVZ023-BD by GreenGate cloning (Lampropoulos *et al.*, 2013). Mutant variants of *SNF4* were generated by site-directed mutagenesis of *SNF4*-AD and verified by sequencing. Phusion high-fidelity DNA polymerase (Thermo Scientific) was used for all PCRs.

For transient expression assays, the *KIN10*, *KIN11* and *SNF4* coding sequences (CDSs) without the stop codon were amplified by PCR from *A. thaliana* Col-0 cDNA and inserted into the HBT95 vector, in-frame with a double haemagglutinin (HA) or a FLAG tag, yellow fluorescent protein (split-YFP) or enhanced green fluorescent protein (GFP) tag (Sheen, 1996). The *DIN6/At3g47340* and *SEN5/AT3G15450* promoter-LUC reporter systems were previously described (Baena-Gonzalez *et al.*, 2007). To obtain the *KIN10* and *SNF4* mutant alleles, plasmid site-directed mutagenesis was performed. To clone the *KIN11* truncated protein coding sequences, we used primers kin11A and kin11cr2B or kin11cr3B. All constructs were confirmed by sequencing. All primers used for cloning are listed in Table S1.

### Transient expression in leaf mesophyll protoplasts

Col-0 plants were grown under a 12 h : 12 h, light : dark diurnal cycle with 75  $\mu\text{E}$  cool white fluorescent light (F17T8/TL741/ALTO; Philips, Eindhoven, the Netherlands) for 4 wk at 21°C. Leaf mesophyll protoplast isolation and transfection were performed as described by Yoo *et al.* (2007). After PEG- $\text{Ca}^{2+}$ -mediated transfection, protoplasts were incubated under dim light (10  $\mu\text{E}$ ) for 6 h for LUC and GUS activity assays and immunoblot analyses or 16 h for GFP localization and bimolecular fluorescence

complementation (BiFC) assays. For statistical analysis, one-way ANOVA and Tukey's HSD test were applied.

### Promoter-LUC activity assays

For LUC and GUS activity assays,  $10^4$  protoplasts were transfected with 10 µg DNA (CsCl gradient-purified), as described in Ramon *et al.* (2019).

### Subcellular localization studies

To observe the subcellular localization of the wild-type and mutant KIN10 proteins,  $4 \times 10^4$  protoplasts were transfected with a total of 30 µg GFP-construct plasmid DNA (CsCl gradient-purified) and 10 µg SC35-like splicing factor 30 (SCF30)-RFP (red fluorescent protein) nuclear DNA marker (CsCl gradient-purified) and incubated for 16 h. GFP and RFP were visualized using confocal laser scanning microscopy (FV1000; Olympus Europe, Hamburg, Germany) with a 40× (oil) objective.

### Bimolecular fluorescence complementation assays

To determine *in vivo* interactions,  $4 \times 10^4$  protoplasts were transfected with a total of 30 µg split-YFP construct plasmid DNA (CsCl gradient-purified) and 10 µg SCF30-RFP nuclear DNA marker (CsCl gradient-purified) and incubated for 16 h. YFP and RFP were visualized using confocal laser scanning microscopy (FV1000; Olympus) with a 40× (1.3 oil) objective.

### Immunoblot analysis

For detection of transiently expressed proteins, protoplasts were transfected with 20 µg DNA (CsCl gradient-purified) and incubated for 6 h, after which 20 µl of loading buffer was added to the protoplast pellet and boiled for 5 min at 95°C. Immunoblotting was performed as described in Ramon *et al.* (2019).

### Yeast-two-hybrid assays

All final AD and BD Y2H constructs were transformed into Y187 and AH109 yeast cells, respectively (Gietz & Schiestl, 2007). Y187 and AH109 cells with the introduced constructs were selected on single synthetic dropout (SD) media without leucine (–L) or tryptophan (–W), respectively. To test the protein binary interactions, the yeast mating system was used according to the Yeast protocols handbook (PT3024-1-Clontech 2001, Palo Alto, CA, USA). Protein–protein interactions were demonstrated by the activation of both HIS and β-galactosidase reporters.

## Results

### Mutations in KIN10 and SNF4 subunits restore flowering in the *tps1-2* mutant

To identify genes that restore flowering and seed set in the non-flowering *tps1-2 GVG::TPS1* mutant, we carried out an EMS

suppressor screen. In total, 106 putative mutants, which suppressed the nonflowering *tps1-2 GVG::TPS1* phenotype and produced seeds, were recovered in the M2 generation.

To identify the causal mutation in one of the suppressor lines, 160-1, the mutant was backcrossed once to *tps1-2 GVG::TPS1*. In total, 180 individual F<sub>2</sub> segregant plants, corresponding to c. 25% of the population, showed the suppressor phenotype (BC1F2) without the application of DEX, and were used for mapping by sequencing. SNP analysis revealed a strong enrichment of EMS-induced SNPs at the top of chromosome 3 in the BC1F2 population of line 160-1 (Fig. 1a). One of the candidate genes containing a nonsynonymous SNP encodes the SnRK1 catalytic subunit KIN10 (At3g01090). As SnRK1 has previously been implicated in T6P signalling (Zhang *et al.*, 2009; Schluemann *et al.*, 2012; Nunes *et al.*, 2013), we considered this mutation as the prime candidate for restoring flowering in the *tps1-2 GVG::TPS1* suppressor line 160-1.

To screen for additional *kin10* alleles, we sequenced the genome of 64 additional suppressor mutants that displayed stable suppression of the *tps1-2* phenotype in the M3 generation (Table S2). After correcting for SNPs that were detected in multiple suppressor lines, 33 513 informative unique SNPs were identified and mapped to the genome (Table S3). From these data we identified three additional suppressor lines (170-1, 199-6, 232-2-1) that carried nonsynonymous amino acid substitutions in *KIN10* (Table S4). Complementation crosses were carried out between three of the potential *kin10* lines, 160-1, 199-6 and 232-2-1. F<sub>1</sub> plants flowered without DEX application, indicating that the three tested suppressor mutants form one complementation group and confirming that the mutations in *kin10* are causal for floral induction in the suppressor lines (Fig. S2). We refer to these new EMS-induced alleles as *kin10-4* (160-1), *kin10-5* (232-2-1) and *kin10-6* (199-6) (Fig. 1b).

Closer examination of the SNP data led to the identification of four potentially deleterious mutations in the SNF4 subunit: three nonsynonymous amino acid substitutions and one potential splice site change (Tables S3, S4). Complementation crosses between two of these potential *snf4* alleles, lines 125-6-1 and 154-1-1, flowered in the F<sub>1</sub> generation without DEX application, suggesting strongly that the mutations in *SNF4* were causal (Fig. S2). We refer to these new EMS-induced *snf4* mutant alleles as *snf4-1* and *snf4-2*, respectively (Fig. 1b).

All *kin10* or *snf4* mutants that were confirmed by complementation assays were backcrossed to *tps1-2 GVG::TPS1* at least once and homozygous suppressor mutant lines were established. Flowering was restored to a similar extent in all the backcrossed lines, except for *snf4-2 tps1-2 GVG::TPS1*, which flowered significantly later than the other suppressor lines (Fig. 1c), indicating that *snf4-2* might be a hypomorphic *SNF4* allele.

Due to the presumed functional redundancy of *KIN10* and *KIN11* (Baena-Gonzalez *et al.*, 2007; Jeong *et al.*, 2015), we investigated whether the loss of a functional *KIN11* subunit also rescues *tps1-2* flowering ability. For this, we created two CRISPR/Cas9 mutant *KIN11* alleles (*kin11cr*) (Fig. S1) and crossed them into both *tps1-2* and *tps1-2 GVG::TPS1* plants. However, we were unable to recover a double *kin11cr tps1-2*

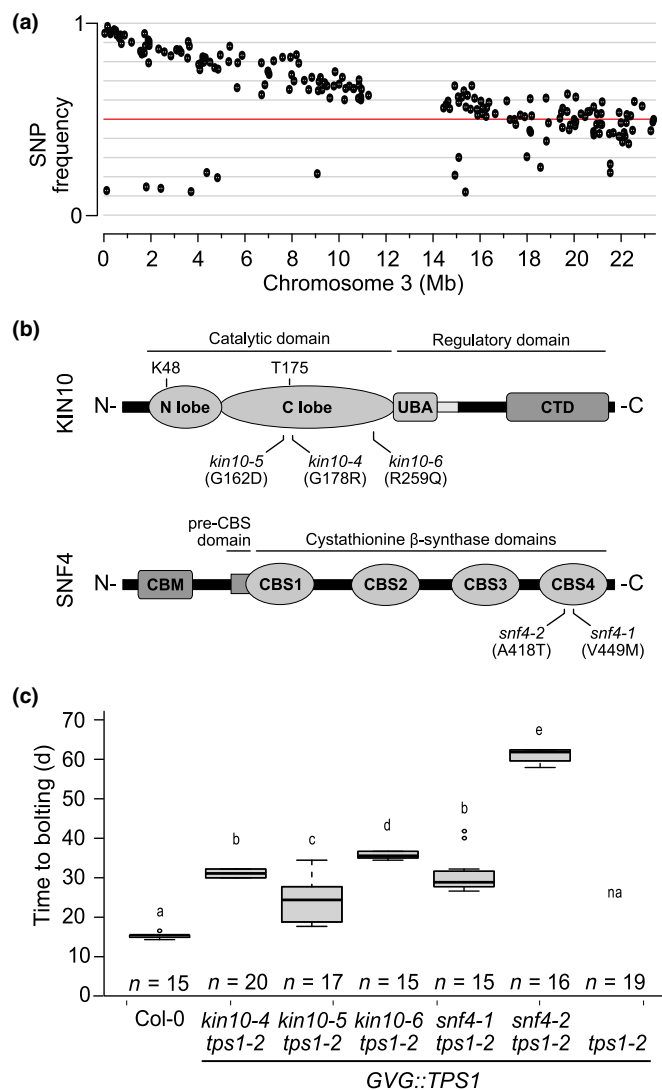


**Fig. 1** Mutations in KIN10 and SNF4 subunits restore flowering in the *Arabidopsis tps1-2* GVG::TPS1 mutant. (a) Frequency of ethyl methanesulfonate (EMS)-induced single nucleotide polymorphisms (SNPs) on chromosome 3 in the BC2F2 population of 160-1 plants. Red line indicates 50% SNP frequency. (b) Schematic representation of the location of the suppressor mutations on the KIN10 and SNF4 proteins. Top: KIN10 protein consisting of a catalytic domain including an N-terminal N-lobe and C-terminal C-lobe, which contain the conserved K48 residue important for phosphotransfer and the T-loop with indicated conserved threonine (T175) residue; a ubiquitin-associated (UBA) domain and linker sequence; and a C-terminal domain (CTD), essential for the complex and other protein–protein interactions. Bottom: the SNF4 protein consisting of an N-terminal carbohydrate-binding module (CBM), a pre-CBS domain, and four cystathionine  $\beta$ -synthase (CBS) domains required for nucleotide binding and complex interactions. Black lines indicate the point mutations identified in this work and the resulting amino acid substitutions in parentheses. (c) Flowering time of EMS suppressor mutants. Plants were grown in LD conditions without dexamethasone application. A one-way ANOVA Tukey's test was applied and letters represent the statistical differences among genotypes ( $P < 0.001$ ), and error bars represent SD;  $n$ , number of individuals; na, not applicable because plants do not flower.

mutant and *kin11cr tps1-2* GVG::TPS1 plants stalled in the vegetative phase, indicating that *kin11cr* mutations neither rescued embryo lethality nor flowering. *kin11cr* plants were

indistinguishable from the wild-type, as already reported for a *kin11* T-DNA knockout line (Jeong *et al.*, 2015). To confirm that the mutant *KIN11cr* alleles do not produce any residual KIN11 activity, we transiently expressed the resulting truncated proteins, lacking a major part of the catalytic domain, in leaf mesophyll protoplasts. As expected, they no longer activate the DIN6-LUC reporter with the *kin11cr2* allele not even producing detectable protein levels, possibly due to nonsense-mediated decay of the transcript and/or instability of the truncated protein (Fig. S1). To summarize, we found that mutations in KIN10 and SNF4, but not in KIN11, can restore flowering in the otherwise nonflowering *tps1-2* GVG::TPS1 background.

### Mutations in KIN10 and SNF4 suppress *tps1-2* embryo lethality

Embryo development in homozygous *tps1-2* plants is arrested at the torpedo stage (Eastmond *et al.*, 2002). Interestingly, embryogenesis is rescued in all the suppressor mutants, including the hypomorphic *snf4-2 tps1-2* GVG::TPS1 mutant. However, these latter mutants produced only very few viable seeds (at most 10 per plant) compared to the other mutants. To exclude the possibility that the observed rescue of flowering and embryogenesis in the suppressor mutants was not caused by inadvertent activation of the GVG::TPS1 transgene, we crossed two of the *kin10* alleles and one of the *snf4* alleles with *tps1-2* heterozygous plants lacking GVG::TPS1. Homozygous mutations in the two SnRK1 subunits were able to restore flowering and embryo development in the homozygous *tps1-2* background (*kin10-4 tps1-2*; *kin10-5 tps1-2*; *snf4-1 tps1-2*), even in the absence of the GVG::TPS1 transgene (Fig. S3c, d). Moreover, the introduction of a previously characterized *kin10* T-DNA insertion, *snrk1 $\alpha$ 1-3* (Mair *et al.*, 2015), into the *tps1-2* mutant restored flowering to a similar extent as the *kin10* alleles recovered from the EMS suppressor screen (Fig. S4). Together, these findings confirm that mutations in both KIN10 and SNF4 can restore embryo development of the *tps1-2* mutant.

Importantly, similar to *snrk1 $\alpha$ 1-3* (Mair *et al.*, 2015), all *kin10* and *snf4* alleles recovered from the EMS suppressor screen were phenotypically indistinguishable from wild-type when introduced into the Col-0 background, indicating that under the conditions tested, single loss-of-function mutations in SnRK1 subunits can only display a phenotype in a sensitized background such as *tps1-2*.

### Induction of flowering of the *tps1-2* mutant by SnRK1 mutations involves both the photoperiod-dependent and age pathways

We observed that apart from the hypomorphic *snf4-2 tps1-2* GVG::TPS1, all *kin10* or *snf4* *tps1-2* GVG::TPS1 double mutants are bolting at 34–38 DAS (Fig. 1c). To determine the time of flowering, we also measured the expression of *API1*, a flower meristem identity gene, in apices of *kin10-5 tps1-2* GVG::TPS1 and *snf4-1 tps1-2* GVG::TPS1 plants. *API1* expression was detectable in wild-type plants starting from 18 DAS and peaked at 22 DAS. In *tps1-2* GVG::TPS1 plants, no induction of *API1*

could be detected. In both double mutants, *API* became detectable only from 22 DAS, and further increased at 34 DAS (Fig. 2c). As expected, *FT* was highly expressed in Col-0 leaves at 14 and 18 DAS (Fig. 2b), preceding *API* expression (Fig. 2c). Surprisingly, even though *FT* expression increased transiently in the double mutants starting at 14 DAS, expression never reached wild-type levels and was very low by the time *API* expression became detectable (Fig. 2b,c). Transient *FT* expression in the suppressor mutants can be explained by upstream *CO* expression

(Fig. 2a), which is at wild-type levels at 14 DAS but drops to close to *tps1-2 GVG::TPS1* levels at later time points. This suggests that although the *CO-FT* module is initially activated in the suppressor mutants, this activation is not maintained and might not be sufficient to complete the transition to flowering. Indeed, we found that the SnRK1 suppressor mutations were capable of inducing flowering in the *ft-10* mutant background (Fig. 2f). Triple mutants flowered later than either *ft-10* or double *kin10-2* and *snf4-1* mutants (Fig. 2f), showing an additive

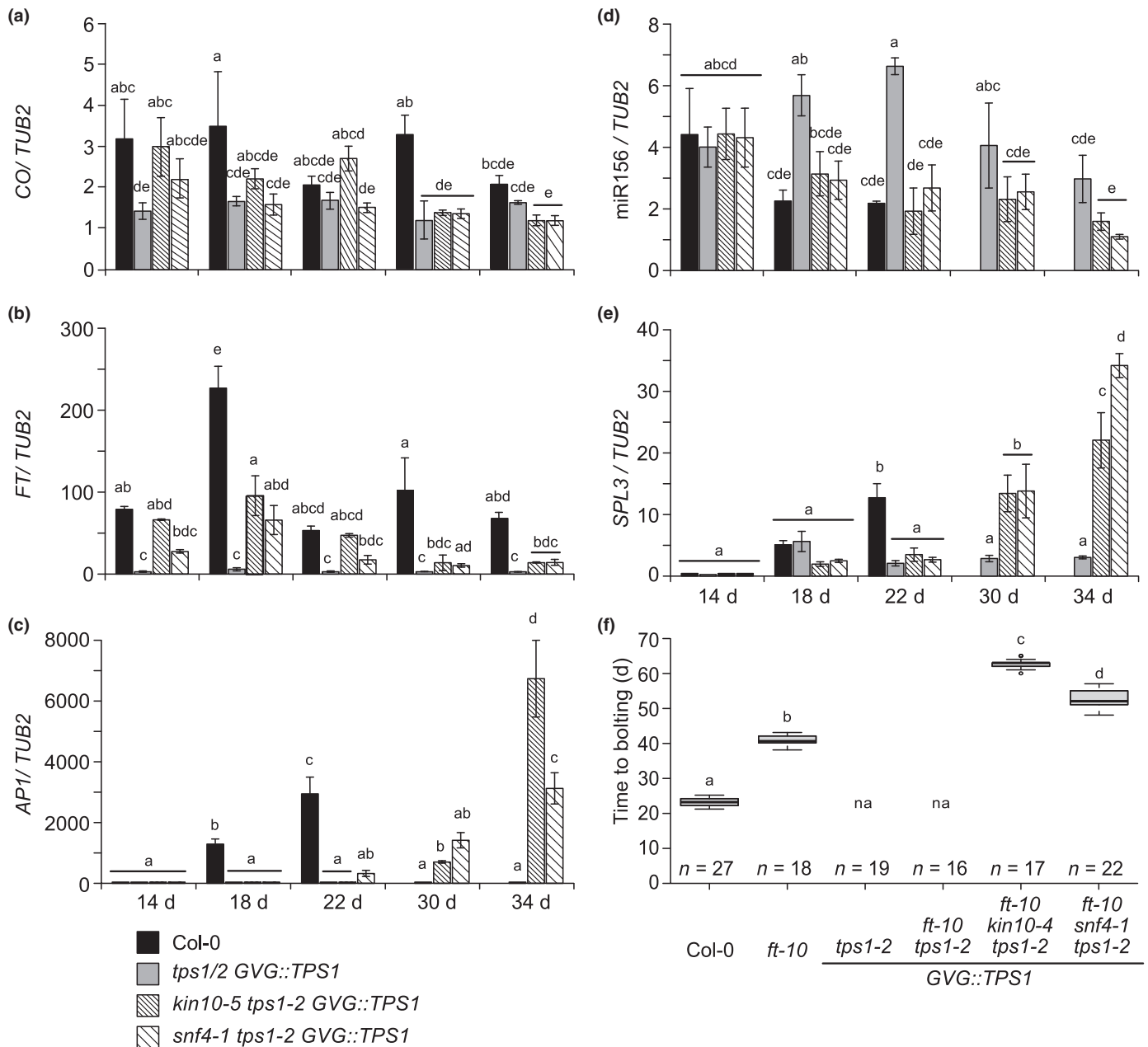


**Fig. 2** Regulation of the age and the photoperiod-dependent pathways is important for SnRK1 to restore flowering in the *Arabidopsis tps1* mutant. (a, b) *CO* (a) and *FT* (b) expression in leaves (whole rosettes) of 14- to 34-d-old plants in long day (LD) conditions. (c, d) Expression of *API* (c), miR156 (d) and *SPL3* (e) in apices of 14- to 34-d-old plants in LD conditions. ANOVA Tukey's multiple comparisons test. Letters a–e represent statistical differences among genotypes and time points. (f) Flowering time of *kin10-5 tps1-2 GVG::TPS1* and *snf4-1 tps1-2 GVG::TPS1* in *ft-10* background under LD conditions. Plants were grown without dexamethasone (DEX) application. ANOVA Tukey's multiple comparisons test. Letters a–d represent the statistical differences among genotypes ( $P < 0.001$ ) and error bars represent SD; n, number of individuals; na, not applicable because plants do not flower.

effect. Expression of the *FT* paralogue *TWIN SISTER OF FT* (*TSF*) was also not significantly restored in the suppressor mutants except for at one time point (Fig. S5). These data suggest that the photoperiod-dependent pathway is involved in initiating the floral transition in the double mutants, but that completion of flowering and bolting may require additional factors.

Likely candidates are miR156 and its targets, the SPL transcription factors, which were previously shown to be compromised in the SAM of *tps1-2 GVG::TPS1* plants (Wahl *et al.*, 2013). In agreement with this, we observed a significantly reduced abundance of miR156 in the suppressor mutants compared to *tps1-2 GVG::TPS1* plants at the time of bolting, 30 and 34 DAS (Fig. 2d), whereas the miR156 target, *SPL3*, was strongly induced (Fig. 2e). Moreover, we observed that the suppressor mutants could flower even under noninductive SD conditions, where the photoperiod pathway is inactive (Fig. S3a,b). This suggests that induction of flowering in the *tps1-2 GVG::TPS1* background by mutations in SnRK1 involves the spatiotemporal activation of both the photoperiod-dependent and the age pathways.

To investigate the effects of *tps1-2* and the suppressor mutations on gene expression in an unbiased way, we carried out a transcriptome analysis using RNA isolated from apices of 18-, 26- and 34-d-old Col-0, *tps1-2 GVG::TPS1*, *kin10-5 tps1-2 GVG::TPS1* and *snf4-1 tps1-2 GVG::TPS1* plants. For Col-0, we collected inflorescences at 26 and 34 DAS because plants had already bolted. Principal component analysis (PCA) indicated that the first component corresponds to developmental changes from a vegetative meristem (Fig. S6a; left), via a transition state, to the inflorescence meristem observed after bolting in 34-d-old Col-0 plants (Fig. S6a; right). Expression of *API* was detected at low levels in Col-0 at 18 DAS while it was barely detectable in *tps1-2 GVG::TPS1* or the suppressor mutants at 18 DAS (Fig. S6b) but became detectable in 26-d-old suppressor mutants and increased further in 34-d-old plants (Fig. S6b), consistent with our RT-qPCR data (Fig. 2c). Similar results were obtained for the B- and C-class genes *APETALA3* (*AP3*) (Fig. S6c), *PISTILLATA* (*Pt*) (Fig. S6d) and *AGAMOUS* (*AG*) (Fig. S6e). The second component, which explains 12% of the variation in that data set, appears to correspond to the age of the plants (Fig. S6a). In this context, it is interesting to note that even though the *tps1-2 GVG::TPS1* mutant does not undergo floral transition, its transcriptome is not static and follows the two suppressor mutants in the PCA plot over time (Fig. S6a).

Because both suppressor mutants showed clear signs of floral transition at 26 DAS in our RNA-seq experiment, further analyses focused on 18-d-old plants. Of the 2040 genes that were significantly differentially expressed between Col-0 and *tps1-2 GVG::TPS1*, 254 were also differentially expressed in *kin10-5 tps1-2 GVG::TPS1* and *snf4-1 tps1-2 GVG::TPS1* when compared to *tps1-2 GVG::TPS1* (Fig. S7; Table S5). Cluster analysis indicated that 175 of these genes were significantly more highly expressed in *tps1-2 GVG::TPS1* than the other three genotypes, whereas expression of 75 genes that were downregulated in *tps1-2 GVG::TPS1* was significantly restored in the suppressor mutants (Fig. S7; Table S5). Among the latter were *SOC1*, *LFY* and *FUL*,

three important flowering time and flower meristem identity genes. Expression of these genes was strongly reduced in the *tps1-2 GVG::TPS1* mutant and significantly restored in both suppressor mutants at 18 DAS and further increased at 26 and 34 DAS (Fig. S6). Since *SOC1* is an early marker of flowering, our RNA-seq data suggest that the suppressor mutants have already initiated the transition to flowering at 18 DAS even though bolting occurs 16–20 d later. To test this hypothesis, we monitored the temporal–spatial expression of *SOC1* in the SAM of plants that were transferred from SD to LD to induce flowering in a synchronized manner. RNA *in situ* hybridization detected transient induction of *SOC1* in the centre of the SAM in Col-0 at the time of floral transition, 3 and 5 d after the shift (Fig. S8). In line with our hypothesis, induction of *SOC1* in the centre of the SAM was weaker but persisted longer in the *snf4-1 tps1-2 GVG::TPS1* mutant before floral primordia became apparent 10 d after the shift. However, *SOC1* expression was confined to the flanks and was not readily detectable in the centre of the SAM in the *kin10-5 tps1-2 GVG::TPS1* mutant at any time point analysed. It would thus appear that mutations in *snf4-2* and *kin10-5*, even though the proteins are part of the same SnRK1 complex, affect spatial expression of *SOC1* differently.

Consistent with our RT-qPCR data, the expression of several miR156 targets was also restored in the suppressor mutants (Fig. S9). Specifically, we found that expression of *SPL3*, *SPL4*, *SPL5* and *SPL15* was strongly increased at later time points (26 and 34 DAS). Notably, the expression of *SPL9*, which has previously been implicated in the regulation of phase transitions (Zhang *et al.*, 2019), was also restored in both mutants (Fig. S9). Together, our results support the idea that the age pathway is required for completion of the floral transition and bolting in the suppressor mutants.

#### *tps1-2* suppressor mutations in *KIN10* affect SnRK1 activity

The observation that single amino acid substitutions in KIN10 can bypass the developmental defects in the *tps1-2 GVG::TPS1* mutant led us to investigate the underlying molecular mechanism. To test whether these mutations are affecting SnRK1 activity, we performed luciferase reporter assays in *A. thaliana* leaf mesophyll protoplasts (Baena-Gonzalez *et al.*, 2007). The mutant versions of the KIN10 protein identified in *kin10-4* (G178R), *kin10-5* (G162D) and *kin10-6* (R259Q) were unable to activate the *SEN5:LUC* and *DIN6:LUC* reporters, similarly to the known inactive KIN10 variants with mutations in key residues of the catalytic domain (K48M) and the kinase T-loop (T175A) (Fig. 3a,b), even though they are efficiently expressed (Fig. 3c) and appropriately localized to the cytoplasm and the nucleus (Fig. 3f).

To further verify that the mutants are impaired in SnRK1 function *in planta*, we analysed expression of the SnRK1 target genes *SEN5* and *DIN6* in response to carbon starvation as a consequence of an artificially extended night. Our results show that the *SEN5* and *DIN6* induction, observed in Col-0 plants, was attenuated in our *kin10* and *snf4* mutants, to a similar extent as in the previously published *kin10* T-DNA insertion line, *snrk1 $\alpha$ -3*

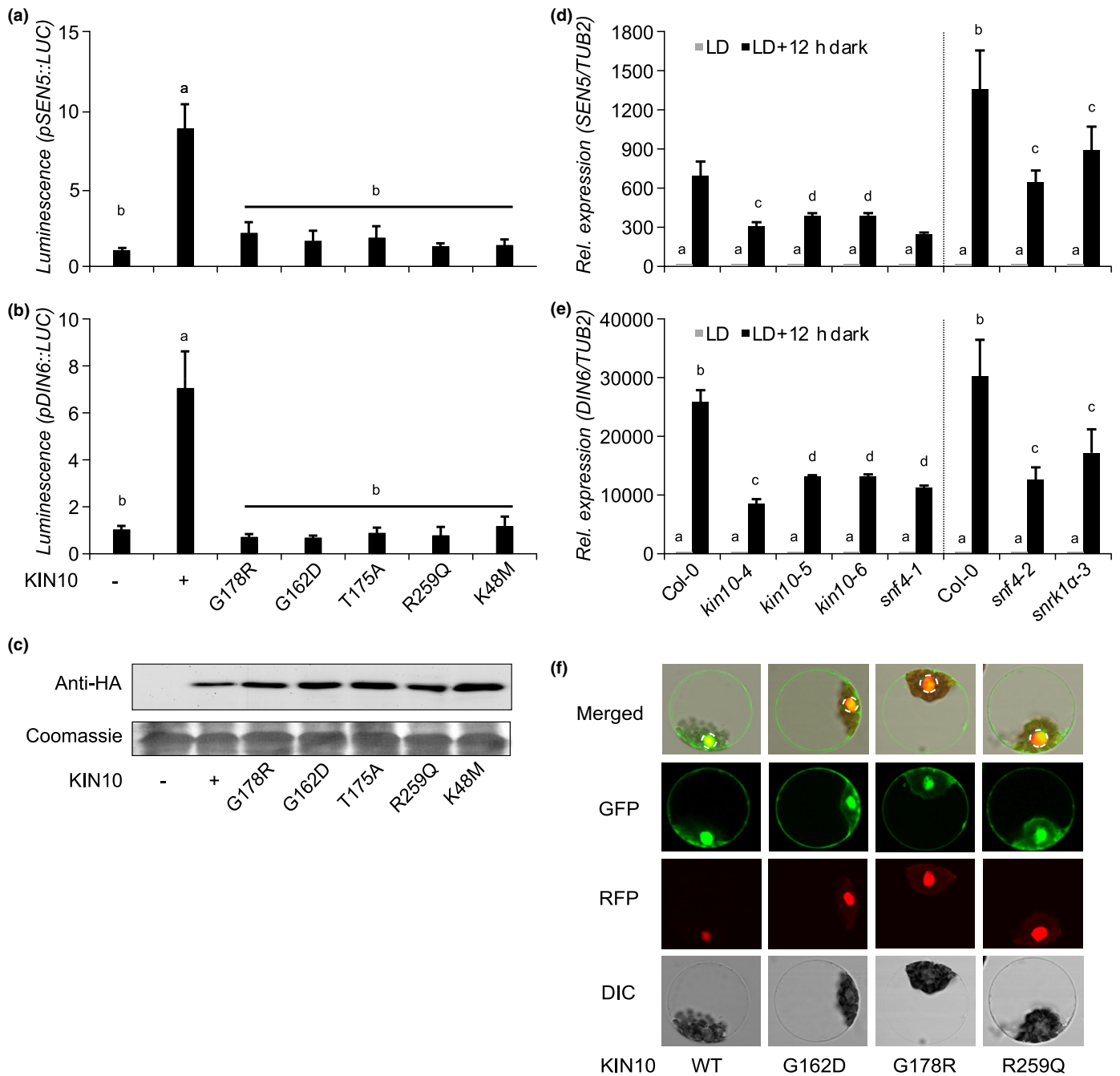


**Fig. 3** Mutations identified in *Arabidopsis* KIN10 and SNF4 result in nonfunctional KIN10 kinase. (a, b) *SEN5* (a) and *DIN6* (b) promoter activity in *Arabidopsis thaliana* leaf protoplasts upon transient expression of wild-type and mutant KIN10 protein versions 6 h after transfection. G178R (*kin10-4*), G162D (*kin10-5*), R259Q (*kin10-6*), K48M (KIN10 catalytic domain) and T175A (KIN10 T-loop). Values are averages with standard deviations ( $n = 4$ ). ANOVA Tukey's multiple comparisons test was applied, letters represent the statistical differences ( $P < 0.001$ ) and error bars represent SD. (c) Protein expression was assessed by immunoblot analysis with anti-HA antibodies. Coomassie staining of Rubisco small subunit (RBCS) served as a loading control. (d, e) *SEN5* (d) and *DIN6* (e) endogenous expression in 14-d-old single *kin10* and *snf4* mutants. LD, long days. Vertical dashed black lines separate the RT-qPCR results of two independent experiments. Error bars represent the SD of three biological replicates. ANOVA Tukey's multiple comparisons test was applied and letters represent the statistical differences among genotypes ( $P < 0.001$ ). (f) Subcellular localization of GFP-tagged KIN10 proteins in *A. thaliana* leaf mesophyll protoplasts. An SCF30-RFP nuclear marker was coexpressed. Dashed circles indicate the nucleus. DIC, differential interference contrast.

(Mair *et al.*, 2015) (Fig. 3d,e). Together, these results indicate that the newly identified mutations, located in the catalytic domain, affect KIN10 activity, whereas the subcellular localization of the mutant proteins appeared to be unaffected when transiently expressed in protoplasts.

*tps1-2* suppressor mutations in SNF4 affect the interaction with KIN10

To the best of our knowledge, no viable *snf4* mutations have been reported. In this study, we identified two mutant *snf4* alleles



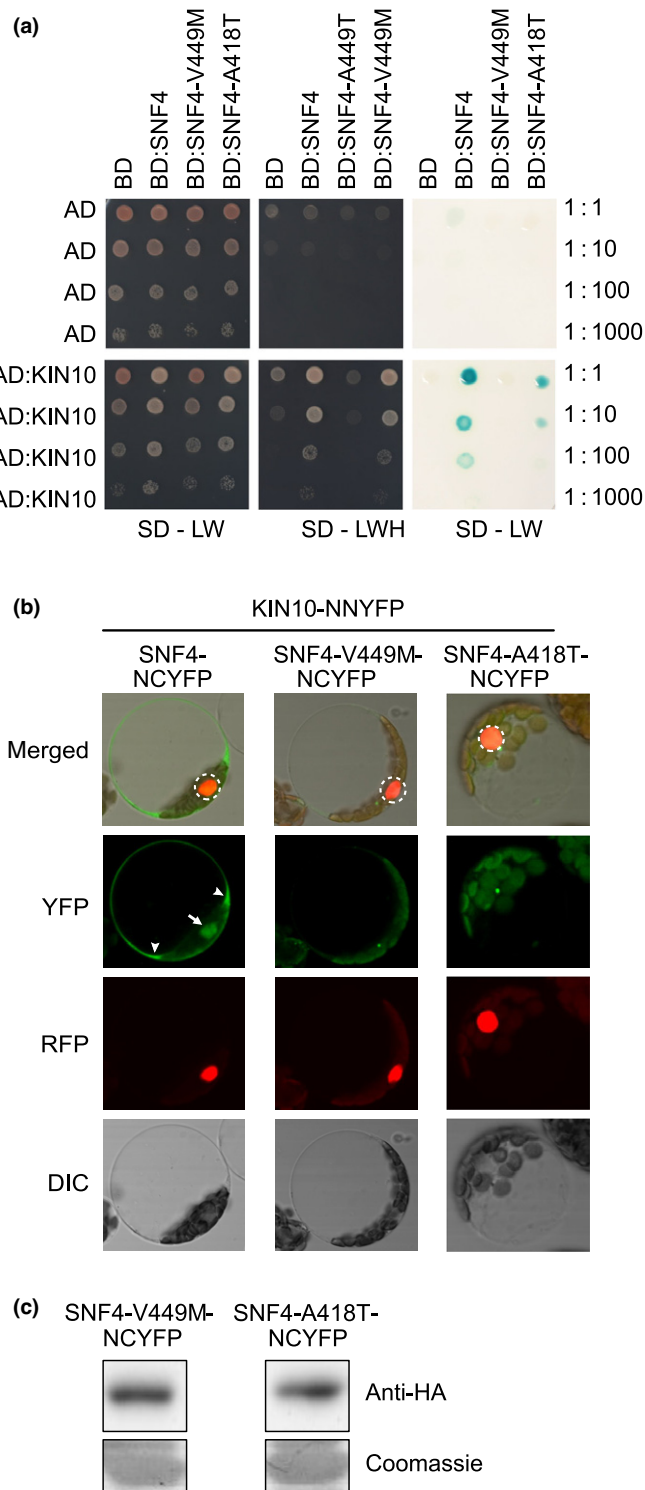
based on their ability to rescue the nonflowering phenotype and suppress embryo lethality of the *tps1-2 GVG::TPS1* mutant. Interestingly, these *snf4* mutations also resulted in reduced SnRK1 signalling activity (Fig. 3d,e). Since SNF4 is a noncatalytic subunit of the SnRK1 complex and the two mutations we identified are both located in the CBS4 domain (Fig. 1b), possibly involved in facilitating complex formation (Gissot *et al.*, 2006; Ramon *et al.*, 2013), we used Y2H and BiFC analysis to test whether the mutations affected the ability of SNF4 to interact with KIN10.

We detected a strong interaction between wild-type SNF4 and KIN10 (Fig. 4a) in yeast, confirming previous results (Kleinow *et al.*, 2000). The interaction was also detectable between KIN10 and the SNF4 variant encoded by the hypomorphic *snf4-2* allele (SNF4-A418T), although the interaction was substantially weaker (Fig. 4a). By contrast, the protein encoded by the strong *snf4-1* allele (SNF4-V449M) was unable to interact with KIN10 (Fig. 4a). These findings are corroborated by results from BiFC assays, which demonstrated that the mutant SNF4 proteins no longer effectively interact with KIN10 in the cytosol or nucleus of leaf cells (Figs 4b, S10) even though they were stably expressed (Fig. 4c). Upon extended exposure, only some small, isolated foci were observed in addition to chloroplast autofluorescence (Figs 4b, S10).

It was recently shown that the KIN $\beta$ 2 subunit can sequester KIN10 in the cytoplasm by myristoylation-dependent membrane association, thereby inhibiting SnRK1 target gene activation. However, SNF4 can antagonize this inhibitory effect, possibly by competing interactions with the catalytic  $\beta$  subunit (Ramon *et al.*, 2019). To test whether loss of the KIN10 interaction with the SNF4 mutant variants (SNF4-A418T and SNF4-V449M) attenuates SnRK1 target gene activation, we coexpressed the SNF4 wild-type and mutant proteins with KIN10 and KIN $\beta$ 2 in *A. thaliana* leaf mesophyll protoplasts and monitored *DIN6*:

**Fig. 4** SNF4 protein mutant versions no longer participate in SnRK1 heterotrimeric complexes. (a) *Arabidopsis* SNF4 protein mutant versions (SNF4-V449M and SNF4-A418T) do not interact or interact weakly with KIN10 in a yeast two-hybrid assay. Yeast colonies were grown in parallel in double dropout media (SD-LW) (left panel) and triple dropout media (SD-LWH) (middle panel) to demonstrate the presence of both bait and prey plasmids (SD-LW) and protein–protein interactions with successful activation of the HIS reporter gene and growth in the absence of histidine (SD-LWH). Right panel: interactions among bait and prey proteins were also confirmed based on expression of the  $\beta$ -galactosidase enzyme, as indicated by the blue colour produced during enzymatic hydrolysis of the X-gal substrate. Three serial dilutions were performed (1 : 10, 1 : 100, 1 : 1000) to show the strength of the interaction. (b) Bimolecular fluorescence complementation (BiFC) assay of the interaction between KIN10 and SNF4, SNF4-V449M or SNF4-A418T upon transient coexpression of the indicated HA-tagged split-YFP constructs, 16 h after transfection. An SCF30-RFP nuclear marker was coexpressed. Dashed circles indicate the nucleus. White arrow and arrowheads mark nuclear and cytoplasmic YFP signals in wild-type SNF4-NCYFP, respectively. DIC, differential interference contrast. (c) Protein expression of the indicated HA-tagged split-YFP constructs was assessed by immunoblot analysis with anti-HA antibodies. Coomassie staining of Rubisco small subunit (RBCS) served as a loading control. NCYFP, N-terminal C-YFP tag.

*LUC* reporter activation. We found that coexpression of wild-type SNF4 indeed relieved KIN $\beta$ 2 repression of KIN10 *DIN6*: *LUC* reporter activation but that the mutant SNF4 proteins were no longer able to do so (Fig. 5). Together, our data suggest that loss of the KIN10–SNF4 interaction is responsible for reduced SnRK1 signalling.



Discussion

T6P and SnRK1 are central players in sensing carbohydrate availability and are essential antagonistic regulators of plant survival, growth and development, including embryogenesis and flowering (Eastmond *et al.*, 2002; Schluempmann *et al.*, 2003; van Dijken *et al.*, 2004; Gomez *et al.*, 2006; Baena-Gonzalez *et al.*, 2007; Wahl *et al.*, 2013). Since it has been shown that *KIN10* and *TPS1* can modulate the circadian clock (Shin *et al.*, 2017; Frank *et al.*, 2018) and that overexpression of *FT* can induce flowering in a *tps1* mutant (Wahl *et al.*, 2013), we expected *FT* expression to be restored in the suppressor mutants. Surprisingly, whereas in wild-type plants the induction of *FT* triggers floral formation within a few days (Fig. 2b), as indicated by *API* expression (Fig. 2c), flowering occurred much later in the suppressor mutants despite an initial transient increase in *FT* expression (Fig. 2b,c). Based on the expression of flowering time and early flower development marker genes, such as *SOC1* and *LFY*, it appears that the floral transition is only moderately delayed in the suppressor mutants (Fig. S6). This idea was confirmed by *SOC1* RNA *in situ* hybridization (Fig. S8), which also revealed surprising differences in the spatial expression of *SOC1* between

the two suppressor mutants. How and why mutations in two subunits of the SnRK1 complex affect *SOC1* patterning differently requires further investigation. Genetic analyses also showed that the suppressor mutations were sufficient to induce flowering in *tps1-2 GVG::TPS1* plants in the absence of a functional *FT* gene (Fig. 2f). Our findings indicate that floral transition is initiated but flower development and bolting are delayed in the suppressor mutants, suggesting the involvement of an additional mechanism.

Flower initiation and bolting are usually synchronized processes but can be uncoupled in early-flowering *A. thaliana* accessions such as C24 and Ler-1 (Miryeganeh *et al.*, 2018). It has also been shown that plant age can induce flowering and bolting in *A. thaliana* (Huijser & Schmid, 2011) and that senescence and bolting are tightly linked processes (Hinckley & Brusslan, 2020). Interestingly, the SnRK1 complex, which promotes catabolic processes to ensure metabolic adaptation for increased cell viability and vitality, is known to affect senescence (Baena-Gonzalez *et al.*, 2007; Kim *et al.*, 2017). For example, overexpression of *KIN10* mimics cellular energy deprivation and delays natural leaf senescence (Baena-Gonzalez *et al.*, 2007; Kim *et al.*, 2017). In addition, *KIN10* directly interacts with and phosphorylates *EIN3*, thus delaying ethylene-promoted organ senescence in plants (Kim *et al.*, 2017). Since the floral transition appears to be extended in our suppressor mutants, and the *miR156/SPL* module, which forms the core of the age pathway, is misregulated in the SAM of the *tps1-2 GVG::TPS1* mutant, we hypothesized that the age pathway is involved in facilitating the timing and length of the floral transition and thus bolting in *A. thaliana*. The finding that at the time of bolting *miR156* levels decrease and expression of several *SPL* genes increases at the SAM (Figs 2d,e, S9) supports this idea. In this context, note that constitutive overexpression of *MIR156* has only a moderate effect on flowering time under LD but it causes extremely late flowering in SD (Schwab *et al.*, 2005). Furthermore, *tps1-2 GVG::TPS1* mutants resemble SD-grown plants in that the expression of *FT* and *TSF* is very much reduced even under LD conditions. This could explain why the moderate decrease of *miR156* and the concomitant increase in *SPLs* have such a pronounced effect on flowering time and bolting in the suppressor mutants. This interpretation is also supported by the observation that the suppressor mutations can induce flowering in the *ft-10* mutant under LD conditions as well as in noninductive SD conditions (Fig. S3a,b).

Moreover, expression of *MIR156a* and *MIR156c* was reported to be repressed by sugars (Yang *et al.*, 2013; Yu *et al.*, 2013), suggesting regulation of the age pathway by the endogenous energy status. In *A. thaliana*, accumulation of sucrose and T6P specifically in LD conditions triggers *FT* expression in leaves to induce flowering (King *et al.*, 2008), and at the time of the floral transition sucrose and T6P accumulate at the SAM (Madhusudanan & Nandakumar, 1983; Komarova & Milyaeva, 1991; Eriksson *et al.*, 2006; Wahl *et al.*, 2013). Thus, the requirement of both the age and the photoperiod pathway in regulating flowering and bolting downstream of the T6P pathway may not be so surprising. However, whereas SnRK1 might control the circadian clock and the photoperiod pathway quite directly (Shin *et al.*,

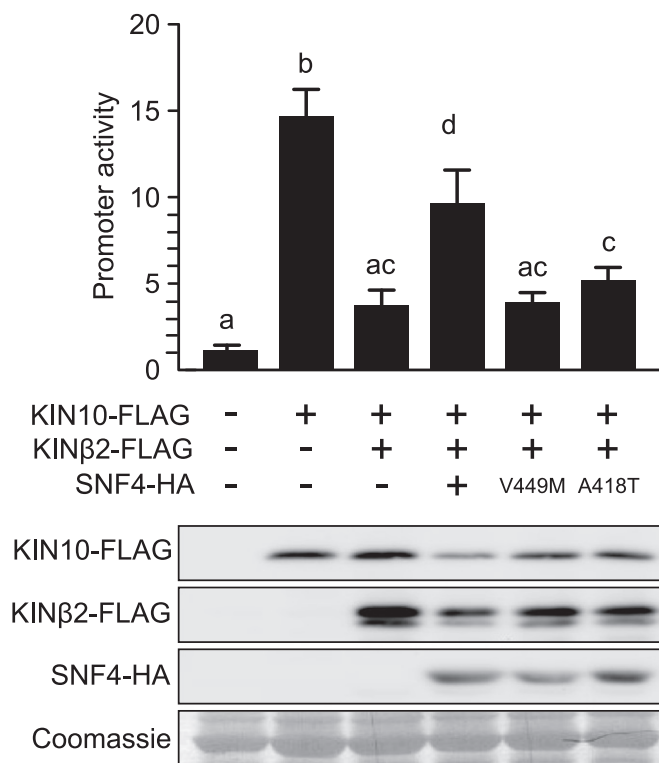


Fig. 5 Mutated SNF4 versions no longer suppress KINβ2 inhibition of KIN10 activity. *DIN6* promoter activity in *Arabidopsis thaliana* leaf mesophyll protoplasts upon transient expression of *Arabidopsis* KIN10, KINβ2 and SNF4 or SNF4-V449M or SNF4-A418T 6 h after transfection. Values are averages with standard deviations (*n* = 4). ANOVA Tukey's multiple comparisons test was applied, and letters represent the statistical differences (*P* < 0.001). Protein expression was assessed by immunoblot analysis with anti-HA and anti-FLAG antibodies. RBSC served as a loading control.

2017; Frank *et al.*, 2018), regulation by the age pathway might be more indirect. Interestingly, a recent study demonstrated that many bolting-associated genes are also expressed during leaf senescence, suggesting that bolting could stimulate senescence-related signalling in mature leaves (Hinckley & Brusslan, 2020). Given that SnRK1 has a negative role in plant ageing and senescence (Baena-Gonzalez *et al.*, 2007; Kim *et al.*, 2017), it is possible that the loss of a functional SnRK1 could trigger the age pathway when the plant ages and thus bolting and flowering completion.

Another interesting observation is that we recovered multiple mutant alleles in *KIN10* from our suppressor screen, but none in *KIN11*. This is unexpected as the two catalytic subunits of SnRK1, KIN10 and KIN11, are often considered functionally redundant. This is based on the observations that single mutants do not display any obvious phenotypes (Jeong *et al.*, 2015), but the double knockout is lethal, and knocking down the expression of both genes causes severe developmental defects (Baena-Gonzalez *et al.*, 2007). A possible explanation is that our genetic screen might not have been saturated or mutations in *KIN11* were missed due to low sequencing coverage. However, a more likely explanation is that *KIN10* and *KIN11* are not fully redundant, a suggestion that is supported by the finding that introducing mutations in *KIN11* in the *tps1-2* or *tps1-2 GVG::TPS1* background was not sufficient to restore embryogenesis or the ability to flower. Together with the observation that overexpression of *KIN10* and *KIN11* have opposing effects on flowering (Williams *et al.*, 2014), our findings suggest strongly that the two genes have only partially overlapping functions.

In contrast to the other SnRK1 subunits, SNF4 is encoded by a single gene in *A. thaliana* (Lumbreras *et al.*, 2001; Gissot *et al.*, 2006) and is essential for plant survival (Ramon *et al.*, 2013; Gao *et al.*, 2016). This suggests that the *snf4* mutants we have identified retain some function. It was recently demonstrated that an interaction with SNF4 is required for KIN10 nuclear activity in the presence of KIN $\beta$ 2, which can retain KIN10 in the cytoplasm through myristoylation-mediated membrane association (Ramon *et al.*, 2019). Interestingly, the point mutations we have identified in SNF4 are located in the last cystathionine  $\beta$ -synthetase domain (CBS4) near the C-terminus, which mediates protein–protein interactions (Fig. 1b). Since the complete loss of function is lethal and nucleotide-binding may not be an important regulatory mechanism in the plant SnRK1 complex, we speculated that the mutated SNF4 proteins may no longer efficiently interact with KIN10. This would also explain why the *snf4* point mutants in many aspects phenocopy *kin10* mutants (Figs 1c, 3a–e). In line with this hypothesis, we observed that the SNF4 mutant proteins did not interact or interacted only weakly with KIN10 (Fig. 4), resulting in reduced nuclear target gene activation in the presence of KIN $\beta$ 2 (Fig. 5). These findings support the idea that the SNF4 interaction is important for KIN10 function and thus essential for SnRK1 energy signalling.

Rather than being activated by low energy stress, the plant SnRK1 kinase appears to be active by default and repressed in energy-rich conditions (Ramon *et al.*, 2019). Consistently, T6P, which functions as a signal for sucrose availability, was identified

as an SnRK1 inhibitor (Zhang *et al.*, 2009). A recent study reported that T6P controls SnRK1 activity by inhibiting the GRIK/SnAK-mediated SnRK1 catalytic subunits' T-loop phosphorylation (Zhai *et al.*, 2018). A prediction from these observations is that high T6P levels in the SAMs of fully developed and photosynthetically active plants and/or LD conditions should repress SnRK1 activity, thereby enabling the transition to flowering and seed set. The finding that suppressor mutations in the KIN10 and SNF4 subunits, which should prevent unrestricted SnRK1 activity, restore flowering and embryogenesis in the *tps1* mutant is in line with this hypothesis. Our results therefore shed light on the connection and opposing roles of T6P and SnRK1 signalling in the metabolic control of plant growth and development, from embryogenesis to flowering.







## Acknowledgements





We thank Johannes Hanson for his critical reading and comments on the manuscript. We thank the UPSC bioinformatics facility (<https://bioinformatics.upsc.se>) for technical support with regard to the RNA-seq data preprocessing and analyses. We would also like to acknowledge support from Uppsala Multidisciplinary Center for Advanced Computational Science for access to the UPPMAX computational infrastructure. We acknowledge funding to the UPSC through grants from VINNOVA and The Knut and Alice Wallenberg Foundation. Work in the Wahl group is supported by the BMBF (031B0191), DFG grants within the SPP1530 (WA3639/1-2, 2-1) and the Max Planck Society. This work was supported by a grant from the Fund for Scientific Research – Flanders (grant FWO G011720N) to FR, a personal fellowship (FWO 11C8819N) to NC and grants from the Deutsche Forschungsgemeinschaft as part of the Priority Program SPP1530 (SCHM1560/8-1, 8-2) and from Vetenskapsrådet (2015-04617) to MS.

## Author contributions

VZ designed and performed most of the experiments; JP performed the EMS suppressor screen, the mapping of suppressor line 160-1 and the low-coverage sequencing of 64 suppressor mutants with help from TL; JH performed the bioinformatics and SNP analyses; NC and FR performed the cellular assays; MM-L and VW performed the RNA *in situ* analysis; NS assisted with the Y2H construct preparation and MS conceived the project; VZ and MS wrote the article with input from all the authors.

## ORCID

Nathalie Crepin  <https://orcid.org/0000-0002-5772-4216>  
 Jörg Hagmann  <https://orcid.org/0000-0002-7232-3103>  
 Tobias Langenecker  <https://orcid.org/0000-0002-9905-7183>  
 Magdalena Musialak-Lange  <https://orcid.org/0000-0002-0388-8960>  
 Jathish Ponnu  <https://orcid.org/0000-0002-3276-7068>  
 Filip Rolland  <https://orcid.org/0000-0003-2601-0752>

Markus Schmid  <https://orcid.org/0000-0002-0068-2967>  
Noemi Skorzinski  <https://orcid.org/0000-0002-1334-385X>  
Vanessa Wahl  <https://orcid.org/0000-0001-7421-8801>  
Vasiliki Zacharaki  <https://orcid.org/0000-0002-5543-2332>

## Data availability

Mapping by sequencing and RNA-seq data are available from ENA, accession nos. PRJEB37882 and PRJEB47979, respectively. Other data supporting the findings of this study are available from the corresponding author upon reasonable request.

## References

- Baena-Gonzalez E, Rolland F, Thevelein JM, Sheen J. 2007. A central integrator of transcription networks in plant stress and energy signalling. *Nature* 448: 938–942.
- Baena-Gonzalez E, Sheen J. 2008. Convergent energy and stress signaling. *Trends in Plant Science* 13: 474–482.
- Broeckx T, Hulsmans S, Rolland F. 2016. The plant energy sensor: evolutionary conservation and divergence of SnRK1 structure, regulation, and function. *Journal of Experimental Botany* 67: 6215–6252.
- Cabib E, Leloir LF. 1958. The biosynthesis of trehalose phosphate. *Journal of Biological Chemistry* 231: 259–275.
- Crozet P, Jammes F, Valot B, Ambard-Bretteville F, Nessler S, Hodges M, Vidal J, Thomas M. 2010. Cross-phosphorylation between *Arabidopsis thaliana* sucrose nonfermenting 1-related protein kinase 1 (AtSnRK1) and its activating kinase (AtSnAK) determines their catalytic activities. *Journal of Biological Chemistry* 285: 12071–12077.
- Delatte TL, Sedijani P, Kondou Y, Matsui M, de Jong GJ, Somsen GW, Wieseklinkenberg A, Primavesi LF, Paul MJ, Schluepmann H. 2011. Growth arrest by trehalose-6-phosphate: an astonishing case of primary metabolite control over growth by way of the SnRK1 signaling pathway. *Plant Physiology* 157: 160–174.
- Dietrich K, Weltmeier F, Ehlert A, Weiste C, Stahl M, Harter K, Droge-Laser W. 2011. Heterodimers of the *Arabidopsis* transcription factors bZIP1 and bZIP53 reprogram amino acid metabolism during low energy stress. *Plant Cell* 23: 381–395.
- van Dijken AJ, Schluepmann H, Smeekens SC. 2004. *Arabidopsis* trehalose-6-phosphate synthase 1 is essential for normal vegetative growth and transition to flowering. *Plant Physiology* 135: 969–977.
- Eastmond PJ, van Dijken AJ, Spielman M, Kerr A, Tissier AF, Dickinson HG, Jones JD, Smeekens SC, Graham IA. 2002. Trehalose-6-phosphate synthase 1, which catalyses the first step in trehalose synthesis, is essential for *Arabidopsis* embryo maturation. *The Plant Journal* 29: 225–235.
- Emanuelle S, Hossain MI, Moller IE, Pedersen HL, van de Meene AM, Doblin MS, Koay A, Oakhill JS, Scott JW, Willats WG *et al.* 2015. SnRK1 from *Arabidopsis thaliana* is an atypical AMPK. *The Plant Journal* 82: 183–192.
- Eriksson S, Bohlenius H, Moritz T, Nilsson O. 2006. GA(4) is the active gibberellin in the regulation of *LEAFY* transcription and *Arabidopsis* floral initiation. *Plant Cell* 18: 2172–2181.
- Estruch F, Treitel MA, Yang X, Carlson M. 1992. N-terminal mutations modulate yeast SNF1 protein kinase function. *Genetics* 132: 639–650.
- Fichtner F, Olas JJ, Feil R, Watanabe M, Krause U, Hoefgen R, Stitt M, Lunn JE. 2020. Functional features of TREHALOSE-6-PHOSPHATE SYNTHASE1, an essential enzyme in *Arabidopsis*. *Plant Cell* 32: 1949–1972.
- Frank A, Mاتيولli CC, Viana AJC, Hearn TJ, Kusakina J, Belbin FE, Wells Newman D, Yochikawa A, Cano-Ramirez DL, Chembath A *et al.* 2018. Circadian entrainment in *Arabidopsis* by the sugar-responsive transcription factor bZIP63. *Current Biology* 28: 2597–2606 e2596.
- Gao XQ, Liu CZ, Li DD, Zhao TT, Li F, Jia XN, Zhao XY, Zhang XS. 2016. The *Arabidopsis* KINβγ subunit of the SnRK1 complex regulates pollen hydration on the stigma by mediating the level of reactive oxygen species in pollen. *PLoS Genetics* 12: e1006228.
- Ghillebert R, Swinnen E, Wen J, Vandesteene L, Ramon M, Norga K, Rolland F, Winderickx J. 2011. The AMPK/SNF1/SnRK1 fuel gauge and energy regulator: structure, function and regulation. *FEBS Journal* 278: 3978–3990.
- Gietz RD, Schiestl RH. 2007. Frozen competent yeast cells that can be transformed with high efficiency using the LiAc/SS carrier DNA/PEG method. *Nature Protocols* 2: 1–4.
- Gissot L, Polge C, Jossier M, Girin T, Bouly JP, Kreis M, Thomas M. 2006. AKINβγ contributes to SnRK1 heterotrimeric complexes and interacts with two proteins implicated in plant pathogen resistance through its KIS/GBD sequence. *Plant Physiology* 142: 931–944.
- Glab N, Oury C, Gueriner T, Domenichini S, Crozet P, Thomas M, Vidal J, Hodges M. 2017. The impact of *Arabidopsis thaliana* SNF1-related-kinase 1 (SnRK1)-activating kinase 1 (SnAK1) and SnAK2 on SnRK1 phosphorylation status: characterization of a SnAK double mutant. *The Plant Journal* 89: 1031–1041.
- Gomez LD, Baud S, Gilday A, Li Y, Graham IA. 2006. Delayed embryo development in the *ARABIDOPSIS* TREHALOSE-6-PHOSPHATE SYNTHASE 1 mutant is associated with altered cell wall structure, decreased cell division and starch accumulation. *The Plant Journal* 46: 69–84.
- Gomez LD, Gilday A, Feil R, Lunn JE, Graham IA. 2010. AtTPS1-mediated trehalose 6-phosphate synthesis is essential for embryogenic and vegetative growth and responsiveness to ABA in germinating seeds and stomatal guard cells. *The Plant Journal* 64: 1–13.
- Hardie DG, Ross FA, Hawley SA. 2012. AMPK: a nutrient and energy sensor that maintains energy homeostasis. *Nature Reviews Molecular Cell Biology* 13: 251–262.
- Hawley SA, Davison M, Woods A, Davies SP, Beri RK, Carling D, Hardie DG. 1996. Characterization of the AMP-activated protein kinase from rat liver and identification of threonine 172 as the major site at which it phosphorylates AMP-activated protein kinase. *Journal of Biological Chemistry* 271: 27879–27887.
- Hedbacker K, Carlson M. 2008. SNF1/AMPK pathways in yeast. *Frontiers in Bioscience* 13: 2408–2420.
- Hedbacker K, Townley R, Carlson M. 2004. Cyclic AMP-dependent protein kinase regulates the subcellular localization of Snf1-Sip1 protein kinase. *Molecular and Cellular Biology* 24: 1836–1843.
- Hinckley WE, Brusslan JA. 2020. Gene expression changes occurring at bolting time are associated with leaf senescence in *Arabidopsis*. *Plant Direct* 4: e00279.
- Huijser P, Schmid M. 2011. The control of developmental phase transitions in plants. *Development* 138: 4117–4129.
- Jeong EY, Seo PJ, Woo JC, Park CM. 2015. AKIN10 delays flowering by inactivating *IDD8* transcription factor through protein phosphorylation in *Arabidopsis*. *BMC Plant Biology* 15: 110.
- Jossier M, Bouly JP, Meimoun P, Arjmand A, Lessard P, Hawley S, Grahame Hardie D, Thomas M. 2009. SnRK1 (SNF1-related kinase 1) has a central role in sugar and ABA signalling in *Arabidopsis thaliana*. *The Plant Journal* 59: 316–328.
- Jumper J, Evans R, Pritzel A, Green T, Figurnov M, Ronneberger O, Tunyasuvunakool K, Bates R, Židek A, Potapenko A *et al.* 2021. Highly accurate protein structure prediction with AlphaFold. *Nature* 596: 583–589.
- Kim GD, Cho YH, Yoo SD. 2017. Regulatory functions of cellular energy sensor SNF1-related kinase1 for leaf senescence delay through ETHYLENE-INSENSITIVE3 repression. *Scientific Reports* 7: 3193.
- King RW, Hisamatsu T, Goldschmidt EE, Blundell C. 2008. The nature of floral signals in *Arabidopsis*. I. Photosynthesis and a far-red photoresponse independently regulate flowering by increasing expression of *FLOWERING LOCUS T (FT)*. *Journal of Experimental Botany* 59: 3811–3820.
- Kleinow T, Bhalerao R, Breuer F, Umeda M, Salchert K, Koncz C. 2000. Functional identification of an *Arabidopsis* Snf4 ortholog by screening for heterologous multicopy suppressors of *snf4* deficiency in yeast. *The Plant Journal* 23: 115–122.
- Komarova EN, Milyaeva EL. 1991. Changes in content and distribution of starch in stem apices of bicolored coneflower during the period of flowering evocation. *Soviet Plant Physiology* 38: 46–51.
- Kong LJ, Hanley-Bowdoin L. 2002. A geminivirus replication protein interacts with a protein kinase and a motor protein that display different expression patterns during plant development and infection. *Plant Cell* 14: 1817–1832.
- Lampropoulos A, Sutikovic Z, Wenzl C, Maegele I, Lohmann JU, Forner J. 2013. GreenGate – a novel, versatile, and efficient cloning system for plant transgenesis. *PLoS ONE* 8: e83043.

- Lumbreras V, Alba MM, Kleinow T, Koncz C, Pages M. 2001. Domain fusion between SNF1-related kinase subunits during plant evolution. *EMBO Reports* 2: 55–60.
- Lunn JE, Delorge I, Figueroa CM, Van Dijk P, Stitt M. 2014. Trehalose metabolism in plants. *The Plant Journal* 79: 544–567.
- Lunn JE, Feil R, Hendriks JH, Gibon Y, Morcuende R, Osuna D, Scheible WR, Carillo P, Hajirezaei MR, Stitt M. 2006. Sugar-induced increases in trehalose 6-phosphate are correlated with redox activation of ADPglucose pyrophosphorylase and higher rates of starch synthesis in *Arabidopsis thaliana*. *Biochemical Journal* 397: 139–148.
- Madhusudan KN, Nandakumar S. 1983. Carbohydrate changes in shoot tip and subtending leaves during ontogenetic development of pineapple. *Zeitschrift Für Pflanzenphysiologie* 110: 429–438.
- Mair A, Pedrotti L, Wurzing B, Anrather D, Simeunovic A, Weiste C, Valerio C, Dietrich K, Kirchner T, Nägeli T *et al.* 2015. SnRK1-triggered switch of bZIP63 dimerization mediates the low-energy response in plants. *eLife* 4: e05828.
- Miryeganeh M, Yamaguchi M, Kudoh H. 2018. Synchronisation of *Arabidopsis* flowering time and whole-plant senescence in seasonal environments. *Scientific Reports* 8: 10282.
- Nunes C, O'Hara LE, Primavesi LF, Delatte TL, Schlupepmann H, Somsen GW, Silva AB, Feveireiro PS, Wingler A, Paul MJ. 2013. The trehalose 6-phosphate/SnRK1 signaling pathway primes growth recovery following relief of sink limitation. *Plant Physiology* 162: 1720–1732.
- Olas JJ, Van Dingenen J, Abel C, Dzialo MA, Feil R, Krapp A, Schlereth A, Wahl V. 2019. Nitrate acts at the *Arabidopsis thaliana* shoot apical meristem to regulate flowering time. *New Phytologist* 223: 814–827.
- Ossowski S, Schneeberger K, Clark RM, Lanz C, Warthmann N, Weigel D. 2008. Sequencing of natural strains of *Arabidopsis thaliana* with short reads. *Genome Research* 18: 2024–2033.
- Polge C, Thomas M. 2007. SNF1/AMPK/SnRK1 kinases, global regulators at the heart of energy control? *Trends in Plant Science* 12: 20–28.
- Ponnu J, Schlereth A, Zacharakis V, Dzialo MA, Abel C, Feil R, Schmid M, Wahl V. 2020. The trehalose 6-phosphate pathway impacts vegetative phase change in *Arabidopsis thaliana*. *The Plant Journal* 104: 768–780.
- Ramon M, Dang TVT, Broeckx T, Hulsmans S, Crepin N, Sheen J, Rolland F. 2019. Default activation and nuclear translocation of the plant cellular energy sensor SnRK1 regulate metabolic stress responses and development. *Plant Cell* 31: 1614–1632.
- Ramon M, Ruelens P, Li Y, Sheen J, Geuten K, Rolland F. 2013. The hybrid four-CBS-domain KINβγ subunit functions as the canonical gamma subunit of the plant energy sensor SnRK1. *The Plant Journal* 75: 11–25.
- Romera-Branchat M, Andres F, Coupland G. 2014. Flowering responses to seasonal cues: what's new? *Current Opinion in Plant Biology* 21: 120–127.
- Satoh-Nagasawa N, Nagasawa N, Malcomber S, Sakai H, Jackson D. 2006. A trehalose metabolic enzyme controls inflorescence architecture in maize. *Nature* 441: 227–230.
- Schlupepmann H, Berke L, Sanchez-Perez GF. 2012. Metabolism control over growth: a case for trehalose-6-phosphate in plants. *Journal of Experimental Botany* 63: 3379–3390.
- Schlupepmann H, Pellny T, van Dijken A, Smeekens S, Paul M. 2003. Trehalose 6-phosphate is indispensable for carbohydrate utilization and growth in *Arabidopsis thaliana*. *Proceedings of the National Academy of Sciences, USA* 100: 6849–6854.
- Schneeberger K, Ossowski S, Lanz C, Juul T, Petersen AH, Nielsen KL, Jorgensen JE, Weigel D, Andersen SU. 2009. SHOREmap: simultaneous mapping and mutation identification by deep sequencing. *Nature Methods* 6: 550–551.
- Schwab R, Palatnik JF, Riester M, Schommer C, Schmid M, Weigel D. 2005. Specific effects of microRNAs on the plant transcriptome. *Developmental Cell* 8: 517–527.
- Sheen J. 1996. Ca<sup>2+</sup>-dependent protein kinases and stress signal transduction in plants. *Science* 274: 1900–1902.
- Shen W, Hanley-Bowdoin L. 2006. Geminivirus infection up-regulates the expression of two *Arabidopsis* protein kinases related to yeast SNF1- and mammalian AMPK-activating kinases. *Plant Physiology* 142: 1642–1655.
- Shen W, Reyes MI, Hanley-Bowdoin L. 2009. *Arabidopsis* protein kinases GRIK1 and GRIK2 specifically activate SnRK1 by phosphorylating its activation loop. *Plant Physiology* 150: 996–1005.
- Shin J, Sanchez-Villarreal A, Davis AM, Du SX, Berendzen KW, Koncz C, Ding Z, Li C, Davis SJ. 2017. The metabolic sensor AKIN10 modulates the *Arabidopsis* circadian clock in a light-dependent manner. *Plant, Cell & Environment* 40: 997–1008.
- Song YH, Shim JS, Kinmonth-Schultz HA, Imaizumi T. 2015. Photoperiodic flowering: time measurement mechanisms in leaves. *Annual Review of Plant Biology* 66: 441–464.
- Srikanth A, Schmid M. 2011. Regulation of flowering time: all roads lead to Rome. *Cellular and Molecular Life Sciences* 68: 2013–2037.
- Vandesteene L, Ramon M, Le Roy K, Van Dijk P, Rolland F. 2010. A single active trehalose-6-P synthase (TPS) and a family of putative regulatory TPS-like proteins in *Arabidopsis*. *Molecular Plant* 3: 406–419.
- Wahl V, Ponnu J, Schlereth A, Arrivault S, Langenecker T, Franke A, Feil R, Lunn JE, Stitt M, Schmid M. 2013. Regulation of flowering by trehalose-6-phosphate signaling in *Arabidopsis thaliana*. *Science* 339: 704–707.
- Weigel D, Glazebrook J. 2002. *Arabidopsis: a laboratory manual*. Cold Spring Harbor, NY, USA: Cold Spring Harbor Laboratory Press.
- Williams SP, Rangarajan P, Donahue JL, Hess JE, Gillaspay GE. 2014. Regulation of sucrose non-fermenting related kinase 1 genes in *Arabidopsis thaliana*. *Frontiers in Plant Science* 5: 324.
- Wingler A, Delatte TL, O'Hara LE, Primavesi LF, Jhurreea D, Paul MJ, Schlupepmann H. 2012. Trehalose 6-phosphate is required for the onset of leaf senescence associated with high carbon availability. *Plant Physiology* 158: 1241–1251.
- Xing HL, Dong L, Wang ZP, Zhang HY, Han CY, Liu B, Wang XC, Chen QJ. 2014. A CRISPR/Cas9 toolkit for multiplex genome editing in plants. *BMC Plant Biology* 14: 327.
- Yadav UP, Ivakov A, Feil R, Duan GY, Walther D, Giavalisco P, Piques M, Carillo P, Hubberten H-M, Stitt M *et al.* 2014. The sucrose-trehalose 6-phosphate (Tre6P) nexus: specificity and mechanisms of sucrose signalling by Tre6P. *Journal of Experimental Botany* 65: 1051–1068.
- Yang HL, Liu YJ, Wang CL, Zeng QY. 2012. Molecular evolution of trehalose-6-phosphate synthase (TPS) gene family in *Populus*, *Arabidopsis* and rice. *PLoS ONE* 7: e42438.
- Yang L, Xu ML, Koo Y, He J, Poethig RS. 2013. Sugar promotes vegetative phase change in *Arabidopsis thaliana* by repressing the expression of *MIR156A* and *MIR156C*. *eLife* 2: e00260.
- Yoo SD, Cho YH, Sheen J. 2007. *Arabidopsis* mesophyll protoplasts: a versatile cell system for transient gene expression analysis. *Nature Protocols* 2: 1565–1572.
- Yu S, Cao L, Zhou CM, Zhang TQ, Lian H, Sun Y, Wu JQ, Huang JR, Wang GD, Wang JW. 2013. Sugar is an endogenous cue for juvenile-to-adult phase transition in plants. *eLife* 2: e00269.
- Zhai Z, Keereetaweep J, Liu H, Feil R, Lunn JE, Shanklin J. 2018. Trehalose 6-Phosphate positively regulates fatty acid synthesis by stabilizing WRINKLED1. *Plant Cell* 30: 2616–2627.
- Zhang H, Zhang L, Han JY, Qian ZY, Zhou BY, Xu YM, Wu G. 2019. The nuclear localization signal is required for the function of *squamosa promoter binding protein-like gene 9* to promote vegetative phase change in *Arabidopsis*. *Plant Molecular Biology* 100: 571–578.
- Zhang Y, Primavesi LF, Jhurreea D, Andralojc PJ, Mitchell RA, Powers SJ, Schlupepmann H, Delatte T, Wingler A, Paul MJ. 2009. Inhibition of SNF1-related protein kinase1 activity and regulation of metabolic pathways by trehalose-6-phosphate. *Plant Physiology* 149: 1860–1871.

## Supporting Information

Additional Supporting Information may be found online in the Supporting Information section at the end of the article.

**Fig. S1** *KIN11* CRISPR/Cas9 mutations.

**Fig. S2** Flowering time of F<sub>1</sub> plants from complementation crosses among *kin10* and *snf4* alleles.

**Fig. S3** Flowering time of suppressor mutants in SD and double mutants in LD lacking the *TPS1* inducible construct.

**Fig. S4** The *kin10* T-DNA line (*snrk1α-3*) rescues *tps1-2* flowering.

**Fig. S5** Relative expression of *TSF* in whole rosettes of 14- to 34-d-old plants.

**Fig. S6** RNA-seq data from Col-0, *tps1-2 GVG::TPS1*, *kin10-5 tps1-2 GVG::TPS1* and *snf4-1 tps1-2 GVG::TPS1* apices.

**Fig. S7** Analysis of significantly differentially expressed genes in 18-d-old plants.

**Fig. S8** Expression of *SOC1* in SAM detected by RNA *in situ* hybridization.

**Fig. S9** Expression of *SPL* genes in apices obtained by RNA-seq.

**Fig. S10** SNF4 protein mutant versions are no longer participating in SnRK1 heterotrimeric complexes.

**Methods S1** Genotyping of *kin10* and *snf4* mutations.

**Methods S2** Mapping of EMS-induced mutations by high-throughput sequencing.

**Methods S3** RT-qPCR information.

**Methods S4** RNA-seq data analyses.

**Methods S5** *SOC1* RNA *in situ* hybridization.

**Table S1** List of oligonucleotides used in this study.

**Table S2** Number of identified SNPs in individual EMS suppressor lines.

**Table S3** Unique SNPs identified in all sequenced EMS suppressor lines.

**Table S4** EMS suppressor lines bearing nonsynonymous mutations in *KIN10* and *SNF4*.

**Table S5** Differentially expressed genes in (a) *tps1-2 GVG::TPS1* vs Col-0, and (b) the suppressor mutants and *tps1-2 GVG::TPS1*.

Please note: Wiley Blackwell are not responsible for the content or functionality of any Supporting Information supplied by the authors. Any queries (other than missing material) should be directed to the *New Phytologist* Central Office.



## About New Phytologist

- *New Phytologist* is an electronic (online-only) journal owned by the New Phytologist Foundation, a **not-for-profit organization** dedicated to the promotion of plant science, facilitating projects from symposia to free access for our Tansley reviews and Tansley insights.
- Regular papers, Letters, Viewpoints, Research reviews, Rapid reports and both Modelling/Theory and Methods papers are encouraged. We are committed to rapid processing, from online submission through to publication 'as ready' via *Early View* – our average time to decision is <23 days. There are **no page or colour charges** and a PDF version will be provided for each article.
- The journal is available online at Wiley Online Library. Visit **www.newphytologist.com** to search the articles and register for table of contents email alerts.
- If you have any questions, do get in touch with Central Office (np-centraloffice@lancaster.ac.uk) or, if it is more convenient, our USA Office (np-usaoffice@lancaster.ac.uk)
- For submission instructions, subscription and all the latest information visit **www.newphytologist.com**